Cycle Polyamide Motif for Recognition of the Minor Groove of DNA

David M. Herman, James M. Turner, Eldon E. Baird, and Peter B. Dervan*

Contribution from the Division of Chemistry and Chemical Engineering, California Institute of Technology, Pasadena, California, 91125

Received September 8, 1998

Abstract: Motifs for covalent linkage of side-by-side complexes of pyrrole−imidazole (Py−Im) polyamides in the DNA minor groove provide for small molecules that specifically recognize predetermined sequences with subnanomolar affinity. Polyamide subunits linked by a turn-specific γ-aminobutyric acid (γ) residue form hairpin polyamide structures. Selective amino-substitution of the prochiral α-position of the γ-turn residue relocates the cationic charge from the hairpin C terminus. Here we report the synthesis of pyrrole resin as well as a solid-phase strategy for the preparation of cycle polyamides. The DNA binding properties of two eight-ring cycle polyamides were analyzed on a DNA restriction fragment containing six base pair match and mismatch binding sites. Quantitative footprint titrations demonstrate that a cycle polyamide of sequence composition cyclo-(γ-ImPyPyPy-(R)$^{H2N}\gamma$-ImPyPyPy-) binds a 5′-AGTACT-3′ site with an equilibrium association constant $K_a = 7.6 \times 10^{10}$ M^{-1}, a 3600-fold enhancement relative to the unlinked homodimer (ImPyPyPy-β-Dp)$_2$·5′-AGTACT-3′, and an 8-fold enhancement relative to hairpin analogue ImPyPyPy-(R)$^{H2N}\gamma$-ImPyPyPy-C3−OH·5′-AGTACT-3′. Replacement of a single nitrogen atom with a C−H (Im→Py) regulates affinity and specificity of the cycle polyamide by 2 orders of magnitude. The results presented here suggest that addition of a chiral γ-turn combined with placement of a second γ-turn within the hairpin structure provides a cycle polyamide motif with favorable DNA binding properties.

Introduction

Small molecules that target predetermined DNA sequences have the potential to control gene expression.[1] Polyamides containing the three aromatic amino acids 3-hydroxypyrrole (Hp), imidazole (Im), and pyrrole (Py) are synthetic ligands that bind to predetermined DNA sequences with subnanomolar affinity.[2,3] DNA recognition depends on a code of side-by-side amino acid pairings oriented N−C with respect to the 5′−3′ direction of the DNA helix in the minor groove.[2−9] An antiparallel pairing of Im opposite Py (Im/Py pair) distinguishes G·C from C·G and both of these from A·T/T·A base pairs.[4] A Py/Py pair binds both A·T and T·A in preference to G·C/C·G.[4,5] The discrimination of T·A from A·T using Hp/Py pairs completes the four base pair (bp) code.[3] The linker amino acid γ-aminobutyric acid (γ) connects polyamide subunits C→N in a "hairpin motif", and these ligands bind to predetermined target sites with >100-fold enhanced affinity relative to dimers.[2,9] In both published and unpublished work, eight-ring hairpin polyamides have been found to regulate transcription and permeate a variety of cell types in culture.[1] *Because topology could*

(1) (a) Gottesfield, J. M.; Nealy, L.; Trauger, J. W.; Baird, E. E.; Dervan, P. B. *Nature* **1997**, *387*, 202−205. (b) Dickenson; L. A., Guzilia; P. Trauger, J. W.; Baird, E. E.; Mosier, D. M.; Gottesfeld, J. M.; Dervan, P. B. *Proc. Natl. Acad. Sci. U.S.A.* **1998**, *95*, 12890.

(2) For subnanomolar binding, see: (a) Trauger, J. W.; Baird, E. E.; Dervan, P. B. *Nature* **1996**, *382*, 559−561. (b) Swalley, S. E.; Baird, E. E.; Dervan, P. B. *J. Am. Chem. Soc.* **1997**, *119*, 6953−6961. (c) Turner, J. M.; Baird, E. E.; Dervan, P. B. *J. Am. Chem. Soc.* **1997**, *119*, 7636−7644. (d) Trauger, J. W.; Baird, E. E.; Dervan, P. B. *Angew. Chem., Int. Ed.* **1998**, *37*, 1421−1423. (e) Turner, J. M.; Swalley, S. E.; Baird, E. E.; Dervan, P. B. *J. Am. Chem. Soc.* **1998**, *120*, 6219−6226.

(3) For Hp/Py pairings, see: (a) White, S. E.; Szewczyk, J. W.; Turner, J. M.; Baird, E. E.; Dervan, P. B. *Nature* **1998**, *391*, 468−471. (b) Kielkopf, C. L.; White, S. E.; Szewczyk, J. W.; Turner, J. M.; Baird, E. E.; Dervan, P. B.; Rees, D. C. *Science* **1998**, *282*, 111.

(4) For specificity of Im/Py pairings, see: (a) Wade, W. S.; Mrksich, M.; Dervan, P. B. *J. Am. Chem. Soc.* **1992**, *114*, 8783−8794. (b) Mrksich, M.; Wade, W. S.; Dwyer, T. J.; Geierstanger, B. H.; Wemmer, D. E.; Dervan, P. B. *Proc. Natl. Acad. Sci. U.S.A.* **1992**, *89*, 7586−7590. (c) Wade, W. S.; Mrksich, M.; Dervan, P. B. *Biochemistry* **1993**, *32*, 11385−11389. (d) Mrksich, M.; Dervan, P. B. *J. Am. Chem. Soc.* **1993**, *115*, 2572−2576. (e) Geierstanger, B. H.; Mrksich, M.; Dervan, P. B.; Wemmer, D. E. *Science* **1994**, *266*, 646−650. (f) Kielkopf, C. L.; Baird, E. E.; Dervan, P. B.; Rees, D. C. *Nat. Struct. Biol.* **1998**, *5*, 104−109. (g) White, S.; Baird, E. E.; Dervan, P. B. *J. Am. Chem. Soc.* **1997**, *119*, 8756−8765.

(5) For Py/Py pairing, see: (a) Pelton, J. G.; Wemmer, D. E. *Proc. Natl. Acad. Sci. U.S.A.* **1989**, *86*, 5723−5727. (b) Pelton, J. G.; Wemmer, D. E. *J. Am. Chem. Soc.* **1990**, *112*, 1393−1399. (c) Chen, X.; Ramakrishnan, B.; Rao, S. T.; Sundaralingham, M. *Nat. Struct. Biol.* **1994**, *1*, 169−175. (d) White, S.; Baird, E. E.; Dervan, P. B. *Biochemistry* **1996**, *35*, 12532−12537.

(6) For Im/Im pairing, see: (a) Geierstanger, B. H.; Dwyer, T. J.; Bathini, Y.; Lown, J. W.; Wemmer, D. E. *J. Am. Chem. Soc.* **1993**, *115*, 4474−4482. (b) Singh, S. B.; Ajay; Wemmer, D. E.; Kollman, P. A. *Proc. Natl. Acad. Sci. U.S.A.* **1994**, *91*, 7673−7677. (c) White, S.; Baird, E. E.; Dervan, P. B. *Chem. Biol.* **1997**, *4*, 569−578.

(7) For H-pin motif, see: (a) Mrksich, M.; Dervan, P. B. *J. Am. Chem. Soc.* **1994**, *116*, 3663. (b) Dwyer, T. J.; Geierstanger, B. H.; Mrksich, M.; Dervan, P. B.; Wemmer, D. E. *J. Am. Chem. Soc.* **1993**, *115*, 9900. (c) Chen, Y. H.; Lown, J. W. *J. Am. Chem. Soc.* **1994**, *116*, 6995. (d) Greenberg, W. A.; Baird, E. E.; Dervan, P. B. *Chem. Eur. J.* **1998**, *4*, 796−805.

(8) For hairpin motif, see: (a) Mrksich, M.; Parks, M. E.; Dervan, P. B. *J. Am. Chem. Soc.* **1994**, *116*, 7983−7988. (b) Parks, M. E.; Baird, E. E.; Dervan, P. B. *J. Am. Chem. Soc.* **1996**, *118*, 6147−6152. (c) Parks, M. E.; Baird, E. E.; Dervan, P. B. *J. Am. Chem. Soc.* **1996**, *118*, 6153−6159. (d) Swalley, S. E.; Baird, E. E.; Dervan, P. B. *J. Am. Chem. Soc.* **1996**, *118*, 8198−8206. (e) Pilch, D. S.; Poklar, N. A.; Gelfand, C. A.; Law, S. M.; Breslauer, K. J.; Baird, E. E.; Dervan, P. B. *Proc. Natl. Acad. Sci. U.S.A.* **1996**, *93*, 8306−8311. (f) de Clairac, R. P. L.; Geierstanger, B. H.; Mrksich, M.; Dervan, P. B.; Wemmer, D. E. *J. Am. Chem. Soc.* **1997**, *119*, 7909−7916.

(9) For polyamide dimers, see: (a) Kelly, J. J.; Baird, E. E.; Dervan, P. B. *Proc. Natl. Acad. Sci. U.S.A.* **1996**, *93*, 6981−6985. (b) Trauger, J. W.; Baird, E. E.; Mrksich, M.; Dervan, P. B. *J. Am. Chem. Soc.* **1996**, *118*, 6160−6166. (c) Geierstanger, B. H.; Mrksich M.; Dervan, P. B.; Wemmer, D. E. *Nat. Struct. Biol.* **1996**, *3*, 321−324. (d) Swalley, S. E.; Baird, E. E.; Dervan, P. B. *Chem. Eur. J.* **1997**, *3*, 1600−1607. (e) Trauger, J. W.; Baird, E. E.; Dervan, P. B. *J. Am. Chem. Soc.* **1998**, *120*, 3534−3535.

10.1021/ja983206x CCC: $18.00 © 1999 American Chemical Society
Published on Web 01/27/1999

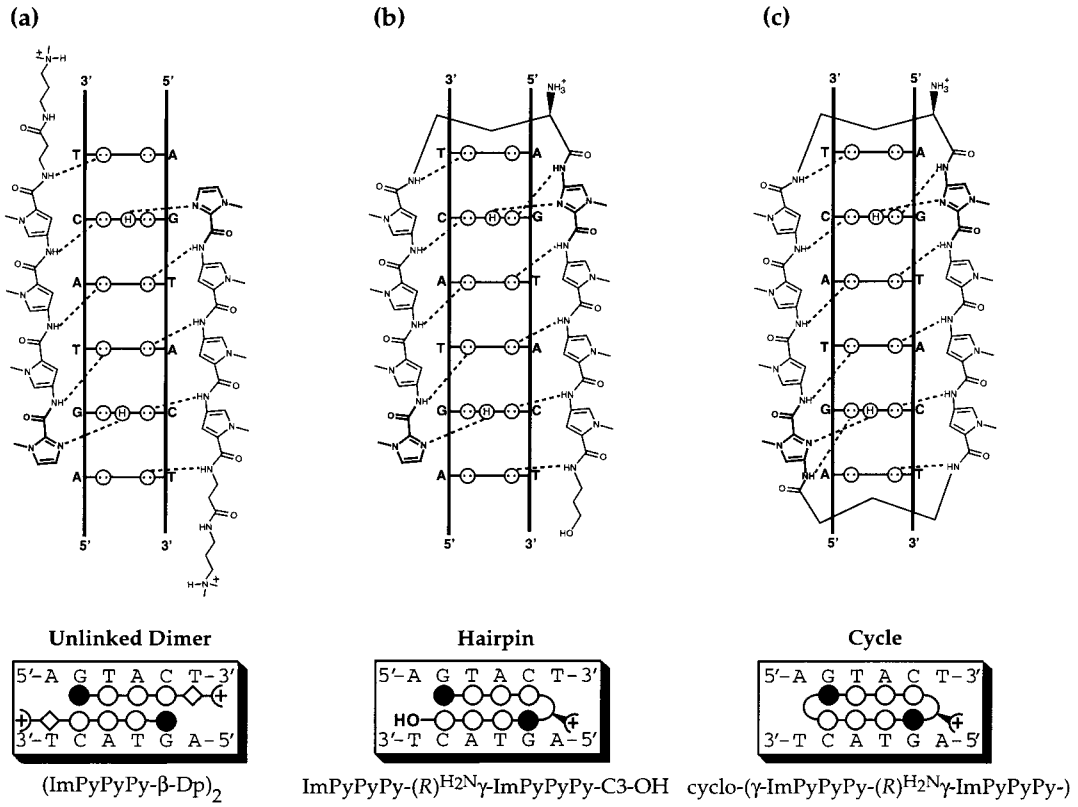

Figure 1. (Top a−c) Hydrogen bond models of the polyamide−DNA complexes formed between the 2:1 dimer ImPyPyPy-β-Dp (**1**), the 1:1 hairpin ImPyPyPy-$(R)^{H2N}\gamma$-ImPyPyPy-OH (**2**), and the 1:1 cyclo-(γ-ImPyPyPy-$(R)^{H2N}\gamma$-ImPyPyPy) (**3**) with the six base pair 5′-AGTACT-3′ match site. Circles with dots represent lone pairs of N3 of purines and O2 of pyrimidines. Circles containing an H represent the N2 hydrogen of G. Putative hydrogen bonds are illustrated by dotted lines. (Bottom a−c) Schematic binding models for **1**, **2**, and **3**. Im and Py rings are represented as shaded and unshaded spheres, respectively.

potentially regulate cell-permeation properties, discovery of new motifs for covalent linkage that provide polyamides with affinities and specificities comparable to naturally occurring DNA binding proteins remains a high priority.

Design of Cycle Polyamides. In a formal sense, addition of a second γ-turn at the C and N termini of a hairpin polyamide allows covalent closure to form a cycle.[10]An initial report described a six-ring (-γ-3-γ-3-) cycle polyamide which bound to a five base pair DNA sequence with higher affinity than a corresponding hairpin polyamide;[10] however, sequence specificity versus mismatch DNA sequences was extremely poor ($\sim$3-fold), compared to 40-fold observed for the hairpin.[11] It was initially thought that the cycle restricted polyamide flexibility, limiting the available conformers to prevent formation of a specific recognition complex. It remained to be determined if γ-turn cycle polyamides could be designed that have comparable DNA binding properties to hairpin-polyamides.

Because of the labor intensive solution-phase cycle polyamide synthesis and the initial discouraging thermodynamics with regard to sequence specificity, the cycle polyamides have not been investigated further until this report. We describe here a pyrrole resin which enables cycle polyamide linear precursors to be synthesized by solid-phase methods, reducing the synthetic effort from weeks to days. Two eight-ring (-γ-4-γ-4-) cycle polyamides have been prepared for the studies described here. Two key design elements from the original six-ring cycle have been altered. First, the number of ring pairings has been increased from three to four. Polyamide−DNA binding affinity is predicted to increase as the number of consecutive ring pairings increases from three to four.[9a] In addition, the charge has been moved from a Py-*N*-methyl group to a γ-turn. Although the detailed effects of the placement of charge remain to be determined, substitution of the prochiral α-position of the γ-turn residue to provide (*R*)-2,4,-diaminobutyric acid has been previously found to yield chiral linked hairpins with enhanced DNA binding sequence specificity and orientation preference.[12] Cycle polyamides must be capped at the N terminus in order to complete the cycle; however, N-terminal acetylation has been found to reduce hairpin-binding specificity and orientation preference.[4g,8b] Analogous to hairpin polyamides, cycle polyamides are capable of forming two mirror image folded structures, one of which is responsible for 5′−3′, N−C match DNA binding[4g] (see Figure 1). It is likely that the chiral amine group could offset the "acetylation effect" by controlling cycle polyamide binding orientation preference and hence binding specificity.[12]

Here we report the DNA binding affinities and sequence specificities of the eight-ring cycle polyamides, cyclo-(γ-ImPyPyPy-$(R)^{H2N}\gamma$-ImPyPyPy-) (**3**) and cyclo-(γ-ImPyPyPy-$(R)^{H2N}\gamma$-PyPyPyPy-) (**4**) that differ by a single amino acid substitution (underlined), for their respective six base pair match sites, 5′-AGTACT-3′ and 5′-AGTATT-3, which differ by a single base pair (underlined). In control experiments, the binding affinity and sequence specificity of the ImPyPyPy-β-Dp (**1**) dimer, and a hairpin analogue ImPyPyPy-$(R)^{H2N}\gamma$-ImPyPyPy-C3−OH (**2**) were also studied (see Figure 2). An EDTA

(10) For cycle polyamides, see: Cho, J. Y.; Parks, M. P.; Dervan, P. B. *Proc. Natl. Acad. Sci. U.S.A.* **1995**, *92*, 10389.

(11) For a review, see: Wemmer, D. E.; Dervan, P. B. *Curr. Opin. Struct. Biol.* **1997**, *7*, 355.

(12) Herman, D. M.; Baird, E. E.; Dervan, P. B. *J. Am. Chem. Soc.* **1998**, *120*, 1382.

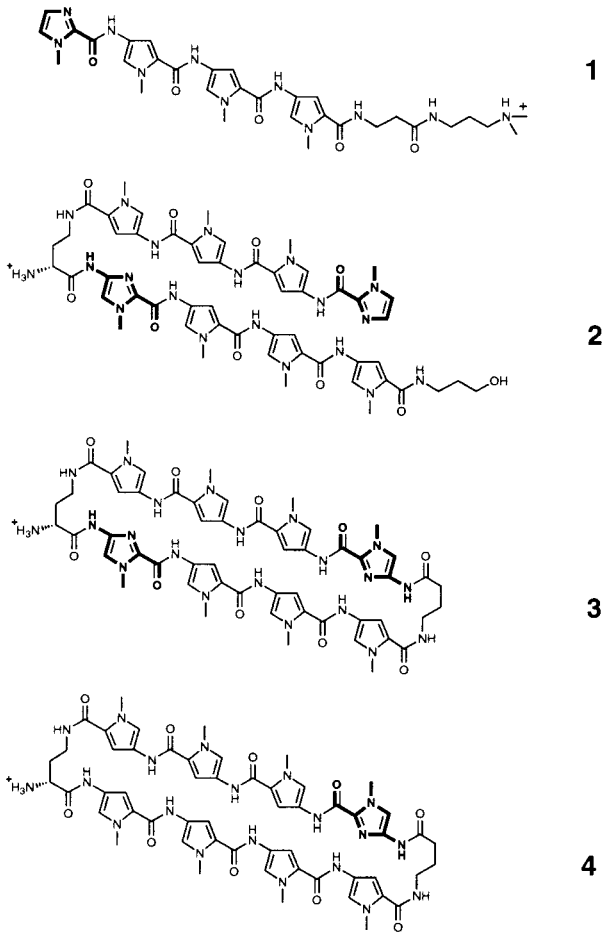

Figure 2. Structures of polyamides ImPyPyPy-β-Dp (**1**), ImPyPyPy-$(R)^{H2N}\gamma$-ImPyPyPy-β-Dp (**2**), ImPyPyPy-$(R)^{H2N}\gamma$-ImPyPyPy-OH (**2**), cyclo-(γ-ImPyPyPy-$(R)^{H2N}\gamma$-ImPyPyPy) (**3**) and cyclo-(γ-ImPyPyPy-$(R)^{H2N}\gamma$-PyPyPyPy) (**4**) as synthesized by solid-phase methods.

analogue cyclo-(γ-ImPyPyPy-$(R)^{EDTA\cdot Fe(II)}\gamma$-PyPyPyPy-) (**4-E·Fe(II)**) was constructed to confirm the binding orientation of cycle polyamide **4** at its 5′-AGTATT-3′ match and 5′-AGTACT-3′ mismatch site. All polyamides were synthesized by solid-phase methods[13] and their purity and identity confirmed by ^{1}H NMR, MALDI-TOF-MS, and analytical HPLC. Precise binding site sizes were determined by MPE·Fe(II) footprinting,[14] and binding orientation and stoichiometry were confirmed by affinity cleaving experiments.[15] Equilibrium association constants (K_a) of the polyamides for respective match and mismatch binding sites were determined by quantitative DNase I footprint titration.[16]

Results and Discussion

Resin Synthesis. The Py-Pam ester (**5**) was prepared according to the published procedures of Merrifield,[17] with Boc-Py acid substituted for the standard Boc protected α-amino acid

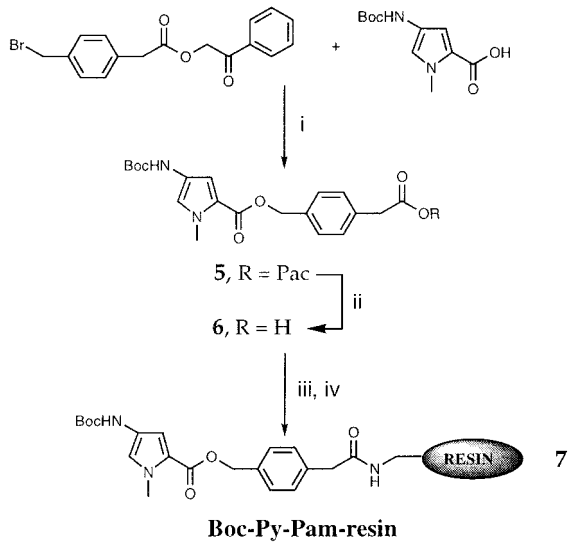

Boc-Py-Pam-resin

Figure 3. Synthesis of Boc-Py-PAM resin (**7**). (i) K_2CO_3, DMF, (ii) Zn/AcOOH (iii) DCC/HOBT, DMF; (iv) aminomethylated-polystyrene; DIEA.

(Figure 3). The phenacyl ester (**5**) was selectively cleaved (Zn, AcOH), and the resultant acid was (**6**) activated (DCC, HOBT) followed by reaction of the activated ester with an excess of 0.7 mmol/g aminomethylated polystyrene for 24 h (DIEA, DMF) to give Boc-Py-Pam resin (**7**). Reactions were stopped at 0.1 mmol/g substitution as determined by quantitative ninhydrin analysis of free amine groups.[18] Unreacted amine groups were capped by acetylation (Ac_2O, DIEA, DMF). Picric acid titration[19] of Py-amino groups was used to verify resin loading of 0.1 mmol/g.

Synthesis of Hairpin Control 2. ImPyPyPy-$(R)^{H2N}\gamma$-ImPyPyPy-β-Pam resin was synthesized by machine-assisted protocols in 18 steps from commercially available Boc-β-Ala-Pam resin (Figure 4a).[13] The polyamide was cleaved from the resin by a single-step reduction with lithium borohydride (EtOH, 60 °C), followed by reversed phase HPLC purification to yield the hairpin polyamide ImPyPyPy-$(R)^{H2N}\gamma$-ImPyPyPy-OH (**2**).

Cycle Polyamide Synthesis. Two polyamide resins, Cbzγ-ImPyPyPy-$(R)^{Fmoc}\gamma$-PyPyPyPy-Pam resin, and Cbzγ-ImPyPyPy-$(R)^{Fmoc}\gamma$-ImPyPyPy-Pam resin were synthesized in 18 steps from Boc-Py-Pam resin (600 mg of resin, 0.1 mmol/g of substitution) using Boc-chemistry machine-assisted protocols (Figure 4b).[13] The (*R*)-2,4-diaminobutyric acid residue was introduced as an orthogonally protected *N*-α-Fmoc-*N*-γ-Boc derivative **10** (HBTU, DIEA). The final step was introduction of Cbzγ-Im acid **11** as a dimer block (HBTU, DIEA).[13] Fmoc-protected polyamide resins Cbzγ-ImPyPyPy-$(R)^{Fmoc}\gamma$-PyPyPyPy-Pam resin, and Cbzγ-ImPyPyPy-$(R)^{Fmoc}\gamma$-ImPyPyPy-Pam resin were treated with 1:4 DMF:piperidine (22 °C, 30 min) to provide Cbzγ-ImPyPyPy-$(R)^{H2N}\gamma$-PyPyPyPy-Pam resin and Cbzγ-ImPyPyPy-$(R)^{H2N}\gamma$-ImPyPyPy-Pam resin, respectively. The amine resins were then treated with Boc-anhydride (DIEA, DMF, 55 °C, 30 min) providing Cbzγ-ImPyPyPy-$(R)^{Boc}\gamma$-PyPyPyPy-Pam resin and Cbzγ-ImPyPyPy-$(R)^{Boc}\gamma$-ImPyPyPy-Pam resin. A single step catalytic transfer hydrogenolysis was used to cleave the polyamide from the solid support and remove the Cbz-protecting group from the N-terminal γ residue. A sample of the resin (240 mg) was treated with palladium acetate (2 mL DMF, 240 mg $Pd(OAc)_2$, 37 °C, 10 min). Ammonium

(13) Baird, E. E.; Dervan, P. B. *J. Am. Chem. Soc.* **1996**, *118*, 6141.
(14) (a) Van Dyke, M. W.; Hertzberg, R. P.; Dervan, P. B. *Proc. Natl. Acad. Sci. U.S.A.* **1982**, *79*, 5470. (b) Van Dyke, M. W.; Dervan, P. B. *Science* **1984**, *225*, 1122.
(15) (a) Taylor, J. S.; Schultz, P. G.; Dervan, P. B. *Tetrahedron* **1984**, *40*, 457. (b) Dervan, P. B. *Science* **1986**, *232*, 464.
(16) (a) Brenowitz, M.; Senear, D. F.; Shea, M. A.; Ackers, G. K. *Methods Enzymol*. **1986**, *130*, 132. (b) Brenowitz, M.; Senear, D. F.; Shea, M. A.; Ackers, G. K. *Proc. Natl. Acad. Sci. U.S.A.* **1986**, *83*, 8462. (c) Senear, D. F.; Brenowitz, M.; Shea, M. A.; Ackers, G. K. *Biochemistry* **1986**, *25*, 7344.
(17) Mitchell, A. R.; Kent, S. B. H.; Engelhard, M.; Merrifield, R. B. *J. Org. Chem.* **1978**, *43*, 2845.
(18) Sarin, V. K.; Kent, S. B. H.; Tam, J. P.; Merrifield, R. B. *Anal. Biochem.* **1981**, *117*, 147.
(19) Gisin, B. F. *Anal. Chim. Acta* **1972**, *58*, 248.

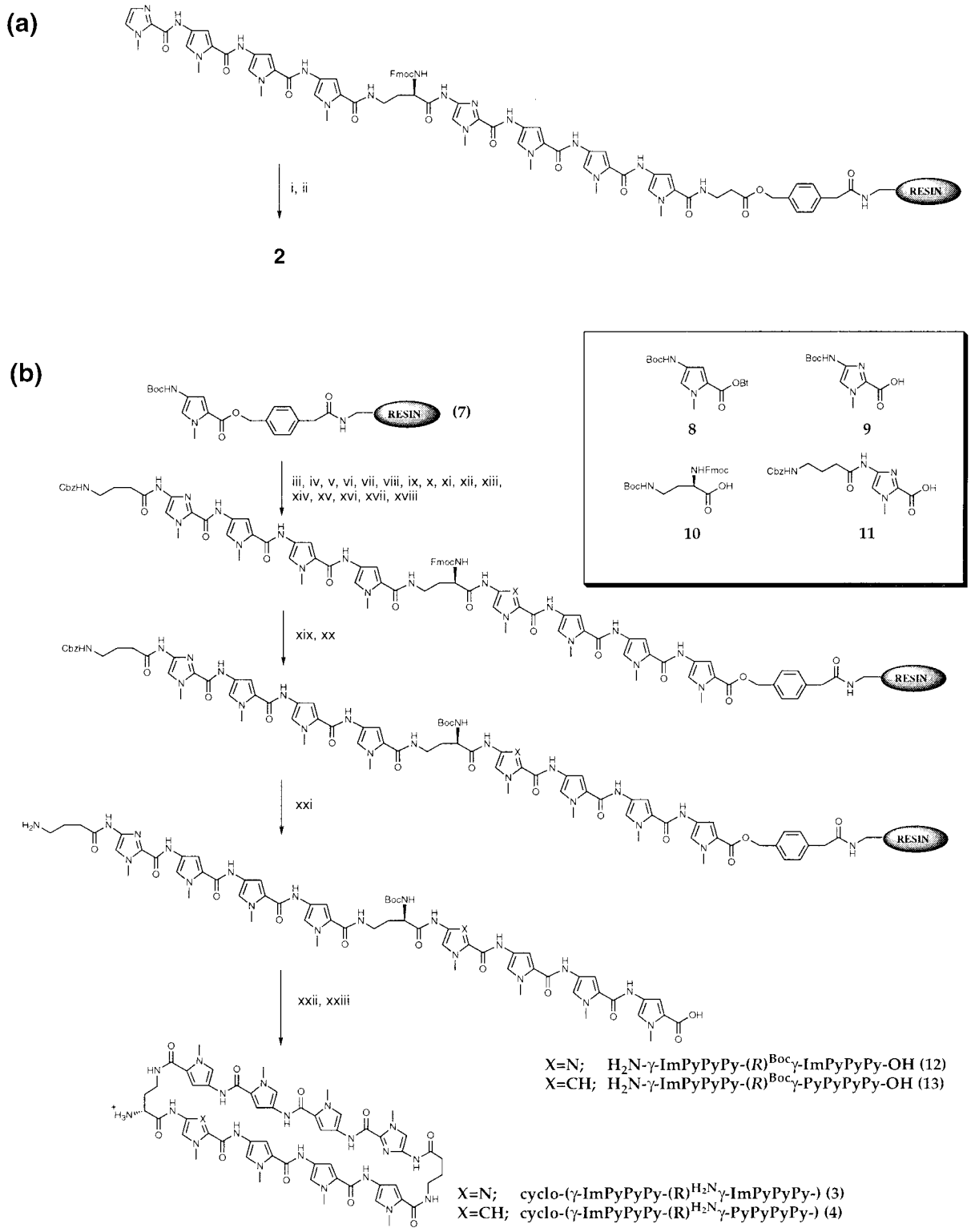

Figure 4. (Box) Monomers for synthesis of compounds described here; Boc-Py-OBt ester **8**, Boc-Im acid **9**, (*R*)-Fmoc-α-Boc-γ-diaminobutyric acid **10**, and Cbz-γ-Im acid **11**. (i) 1:4 DMF/piperidine (22 °C, 30 min): (ii) LiBH4, EtOH, reflux 16 h. (iii) 80% TFA/DCM, 0.4 M PhSH; (iv) Boc-Py-OBt, DIEA, DMF; (v) 80% TFA/DCM, 0.4 M PhSH; (vi) Boc-Py-OBt, DIEA, DMF; (vii) 80% TFA/DCM, 0.4 M PhSH; (viii) Boc-Im acid (DCC, HOBT) for **3**, Boc-Py-OBt, DIEA, DMF for **4**; (ix) 80% TFA/DCM, 0.4 M PhSH; (x) (*R*)-Fmoc-α-Boc-γ-diaminobutyric acid (HBTU, DIEA); (xi) 80% TFA/DCM, 0.4 M PhSH; (xii) Boc-Py-OBt, DIEA, DMF; (xiii) 80% TFA/DCM, 0.4 M PhSH; (xiv) Boc-Py-OBt, DIEA, DMF; (xv) 80% TFA/DCM, 0.4 M PhSH; (xvi) Boc-Py-OBt, DIEA, DMF; (xvii) 80% TFA/DCM, 0.4 M PhSH; (xviii) Cbz-γ-Im acid (HBTU, DIEA); (xix) 80% Piperdine/DMF (25 °C, 30 min); (xx) Boc-anhydride, DIEA, DMF; (xxi) $Pd(OAc)_2$, HCO_2NH_4, DMF (37 °C, 8 h); (xxii) DPPA, K_2CO_3 (xxiii) TFA (1 h). (Inset) Pyrrole, imidazole, and diaminobutyric acid monomers for solid-phase synthesis: Boc-Pyrrole-OBt ester[13] (Boc-Py-OBt) (**8**), imidazole-2-carboxylic acid[4a] (Im-OH) (**9**), (*R*)-Fmoc-α-Boc-γ-diaminobutyric acid (**10**), and CBZ-γ-aminobutyric acid-imidazole dimer (**11**).

formate was added (500 mg, 8 h) and the reaction mixture purified by reversed phase HPLC to provide H_2N-γ-ImPyPyPy-$(R)^{Boc}$γ-PyPyPyPy-COOH (**13**) and H_2N-γ-ImPyPyPy-$(R)^{Boc}$γ-ImPyPyPy-COOH (**12**). Cyclization of H_2N-γ-ImPyPyPy-$(R)^{Boc}$γ-PyPyPyPy-COOH (**13**) and H_2N-γ-ImPyPyPy-$(R)^{Boc}$γ-ImPyPyPy-COOH (**12**) was achieved with DPPA and potassium

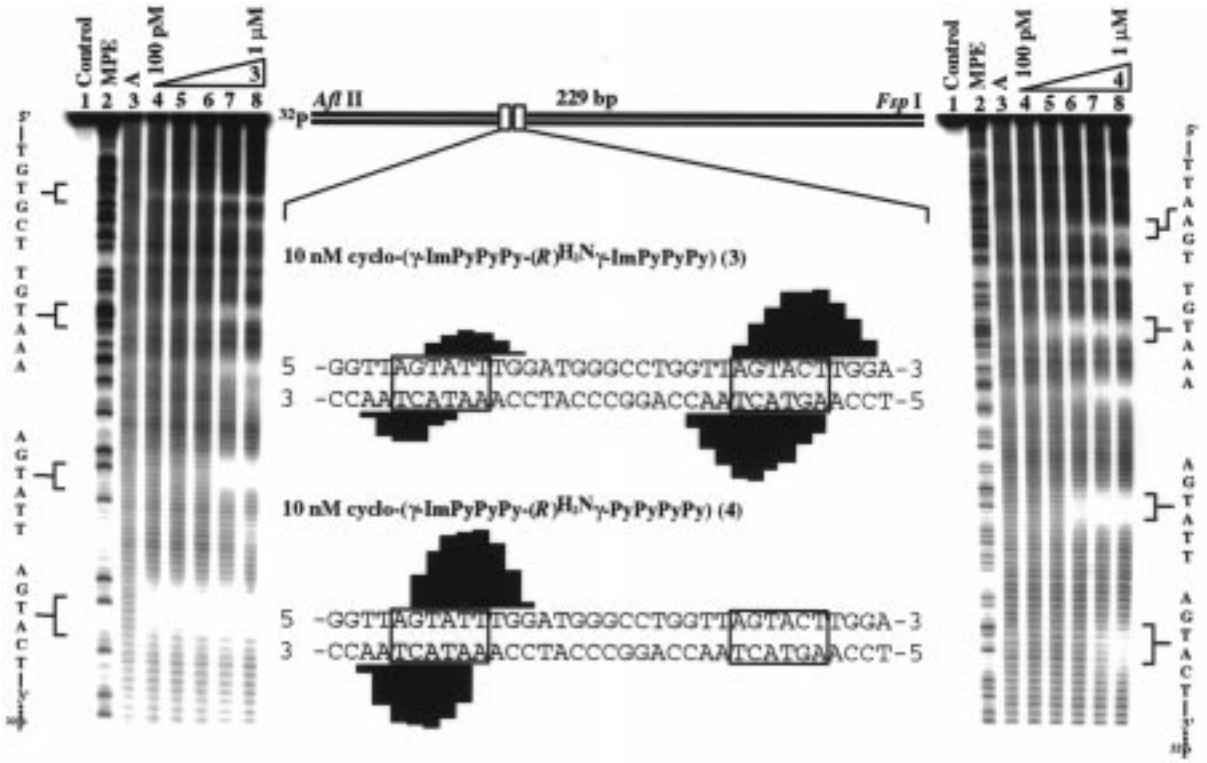

Figure 5. (Middle) Illustration of the 229 base pair restriction fragment with the position of the sequence indicated. MPE·Fe(II) protection patterns of 10 nM cyclo-(γ-ImPyPyPy-(R)$^{H2N}\gamma$-ImPyPyPy) (**3**) and 10 nM cyclo-(γ-ImPyPyPy-(R)$^{H2N}\gamma$-PyPyPyPy) (**4**). Bar heights are proportional to the relative protection from cleavage at each band. Binding sites determined by MPE·Fe(II) footprinting are boxed. MPE·Fe(II) footprinting experiments of cyclo-(γ-ImPyPyPy-(R)$^{H2N}\gamma$-ImPyPyPy) (**3**) (left) and cyclo-(γ-ImPyPyPy-(R)$^{H2N}\gamma$-PyPyPyPy) (**4**) (right) on the 3′ ^{32}P-labeled 229 bp restriction fragment of pJT8. 5′-AGTATT-3′ and 5′-AGTACT-3′ sites are shown adjacent to the autoradiograms. Additional 5′-TGTAAA-3′, 5′-TGTGCT-3′, and 5′-TTAAGT-3′ mismatch sites are not analyzed. Lane 1, intact; lane 2, A reaction; lane 3, MPE·Fe(II) standard; lanes 4−8, 100 pM, 1 nM, 10 nM, 100 nM and 1 μM polyamide. All lanes contain 15 kcpm of either 3′- or 5′-radiolabeled DNA, 25 mM HEPES buffer (pH 7.3), 200 mM NaCl, 50 mg/mL glycogen, 5 mM DTT, and 0.5 mM MPE·Fe(II), 22 °C.

carbonate, as described previously.[10] The Boc-protecting group was then removed in situ by treatment with neat TFA to yield the cyclic compounds cyclo-(γ-ImPyPyPy-(R)$^{H2N}\gamma$-ImPyPyPy-) (**3**) and cyclo-(γ-ImPyPyPy-(R)$^{H2N}\gamma$-PyPyPyPy-) (**4**) after subsequent purification by reversed phase HPLC. The cycle polyamides are obtained with similar yield and purity and have similar solubility as their hairpin counterparts.

Binding Site Size. MPE·Fe(II) footprinting[14] on 3′- or 5′-^{32}P end-labeled 229 base pair restriction fragments reveals that each cycle polyamide, at 10 nM concentration, binds to its designated six base pair match sites (25 mM HEPES buffer (pH 7.3), 200 mM NaCl, 50 μg/mL glycogen, 5 mM DTT, 0.5 μM MPE·Fe(II), and 22 °C) (Figure 5). The polyamide cyclo-(γ-ImPyPyPy-(R)$^{H2N}\gamma$-ImPyPyPy-) (**3**) which contains an Im/Py and a Py/Im pair, protects the cognate 5′-AGTACT-3′ match site. Binding of the single base pair mismatch site 5′-AGTATT-3′ is only seen at much higher polyamide concentrations. The polyamide cyclo-(γ-ImPyPyPy-(R)$^{H2N}\gamma$-PyPyPyPy-) (**4**) which contains a single Im/Py pair protects the designated match site 5′-AGTATT-3′ and the single base pair mismatch site 5′-AGTACT-3′. The sizes of the asymmetrically 3′-shifted footprint cleavage patterns are consistent with 1:1 cycle polyamide/DNA complex formation at six base pair binding sites.

Binding Orientation. Affinity cleavage experiments[15] using cyclo-(γ-ImPyPyPy-(R)$^{EDTA\cdot Fe(II)}\gamma$-PyPyPyPy-) (**4-E·Fe(II)**), which has an EDTA·Fe(II) moiety appended to the γ-turn, were used to confirm polyamide binding orientation and stoichiometry. For synthesis of the EDTA analogue, cyclo-(γ-ImPyPyPy-(R)$^{H2N}\gamma$-PyPyPyPy-) (**4**) was treated with an excess of EDTA-dianhydride (DMSO/NMP, DIEA, 55 °C, 15 min) and the remaining anhydride was hydrolyzed (0.1 M NaOH, 55 °C, 10 min). Cyclo-(γ-ImPyPyPy-(R)$^{EDTA}\gamma$-PyPyPyPy-) (**4-E·Fe(II)**) was then isolated by reversed phase HPLC (Figure 6a). Affinity cleavage experiments were performed on the same 3′- or 5′-^{32}P end-labeled 229 base pair DNA restriction fragment from the plasmid pJT8 (20 mM HEPES buffer (pH 7.3), 200 mM NaCl, 50 μg/mL glycogen, 5 mM DTT, 1 μM Fe(II), pH 7.0 and 22 °C). The observed cleavage pattern for cyclo-(γ-ImPyPyPy-(R)$^{EDTA\cdot Fe(II)}\gamma$-PyPyPyPy) (**4-E·Fe(II)**) (Figure 6b and c) are 3′-shifted, consistent with minor groove occupancy. In the presence of 100 nM **4-E·Fe(II)**, a major cleavage locus proximal to the 3′-side of the 5′-AGTATT-3′ match sequence is revealed, consistent with formation of an oriented 1:1 cycle polyamide−DNA complex. At the same ligand concentration, minor cleavage loci located 3′ and 5′ adjacent to the single base pair mismatch 5′-AGTACT-3′ site appear, consistent with dual binding orientations at this symmetrical binding site. The cyclo-polyamide binding model is further supported by the location of cleavage loci at the 5′-side of the 5′-AGTATT-3′ match site (Figure 6c), and at the 5′- and 3′- sides of the 5′-AGTACT-3′ mismatch site corresponding to the EDTA·Fe(II) moiety placement off the ((R)$^{H2N}\gamma$)-turn residue.

Binding Energetics. Quantitative DNase I footprint titrations[16] (10 mM Tris·HCl, 10 mM KCl, 10 mM $MgCl_2$, and 5 mM $CaCl_2$, pH 7.0, and 22 °C) were performed to determine the equilibrium association constants (K_a) of ImPyPyPy-β-Dp (**1**), ImPyPyPy-(R)$^{H2N}\gamma$-ImPyPyPy-OH (**2**), cyclo-(γ-ImPyPyPy-(R)$^{H2N}\gamma$-ImPyPyPy) (**3**), and cyclo-(γ-ImPyPyPy-(R)$^{H2N}\gamma$-PyPyPyPy) (**4**) for the six base pair match and mismatch sites (Table 1 and Figure 7). Polyamide **1** binds the respective match

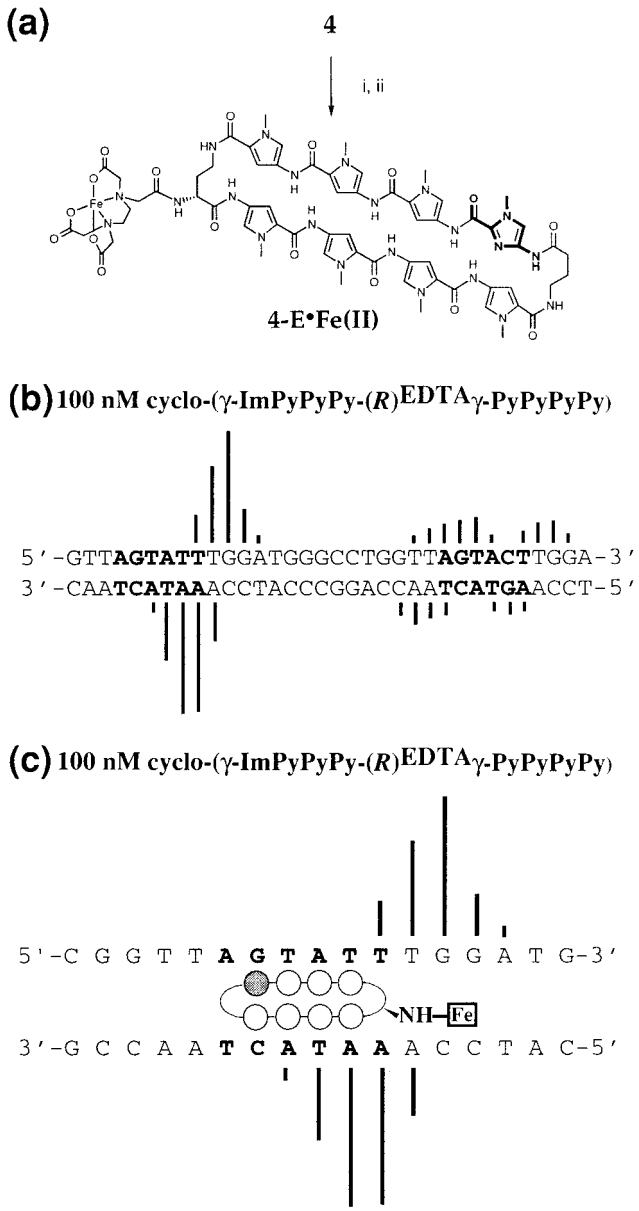

Figure 6. (a) Synthesis of **4-E·Fe(II)**: (i) EDTA dianhydride (DMSO/NMP, DIEA, 55 °C, 15 min); (ii) 0.1 M NaOH (55 °C, 10 min). (b) Affinity cleavage pattern for cyclo-(γ-ImPyPyPy-(*R*)$^{EDTA\cdot Fe(II)}$γ-PyPyPyPy) (**4-E·Fe(II)**) at 100 nM concentration depicting a single binding orientation at the 5′-AGTATT-3 match site and no orientational preference at the 5′-AGTACT-3′ mismatch site. (c) Ball-and-stick model of **4-E·Fe(II)**·5′AGTATT-3′ complex. Bar heights are proportional to the relative cleavage intensities at each base pair. Shaded and nonshaded circles denote imidazole and pyrrole carboxamides, respectively. The boxed Fe denotes the EDTA·Fe(II) cleavage moiety. See Supporting Information for autoradiograms.

and mismatch sites with binding isotherms consistent with 2:1 dimer formation.[12,23] Hairpin polyamide (**2**) and cycle polyamides (**3**) and (**4**) bind their respective match and mismatch sequences with binding isotherms consistent with binding in a 1:1 polyamide−DNA complex.[12,23] Polyamides bind the 5′-AGTACT-3′ site with decreasing affinity; match cycle (**3**) > match hairpin (**2**) > mismatch cycle (**4**) > match dimer (**1**). Polyamides bind the 5′-AGTATT-3′ sequence with decreasing affinity; match cycle (**4**) > mismatch cycle (**3**) > mismatch hairpin (**2**) > mismatch dimer (**1**).

Table 1. Association Constants (M^{-1}) for Polyamides **1**−**4**[a−d]

Polyamide		Motif	5′-AGTACT-3′	5′-AGTATT-3′	Specificity
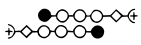	**1**	dimer	$\mathbf{K_a = 2.1 \times 10^7}$	$K_a = 1.4 \times 10^6$	15
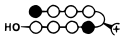	**2**	hairpin	$\mathbf{K_a = 9.0 \times 10^9}$	$K_a = 5.0 \times 10^8$	18
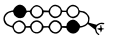	**3**	cycle	$\mathbf{K_a = 7.6 \times 10^{10}}$	$K_a = 1.3 \times 10^9$	55
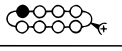	**4**	cycle	$K_a = 4.2 \times 10^8$	$\mathbf{K_a = 3.1 \times 10^9}$	0.14

[a] The reported equilibrium association constants are the mean values obtained from three DNase I footprint titration experiments. [b] The assays were carried out at 22 °C, pH 7.0 in the presence of 10 mM Tris·HCl, 10 mM KCl, 10 mM $MgCl_2$, and 5 mM $CaCl_2$. [c] Apparent monomer association constants were determined for polyamide homodimers.[23] [d] Specificity calculated as K_a(5′-AGTACT-3′)/K_a(5′-AGTATT-3′).

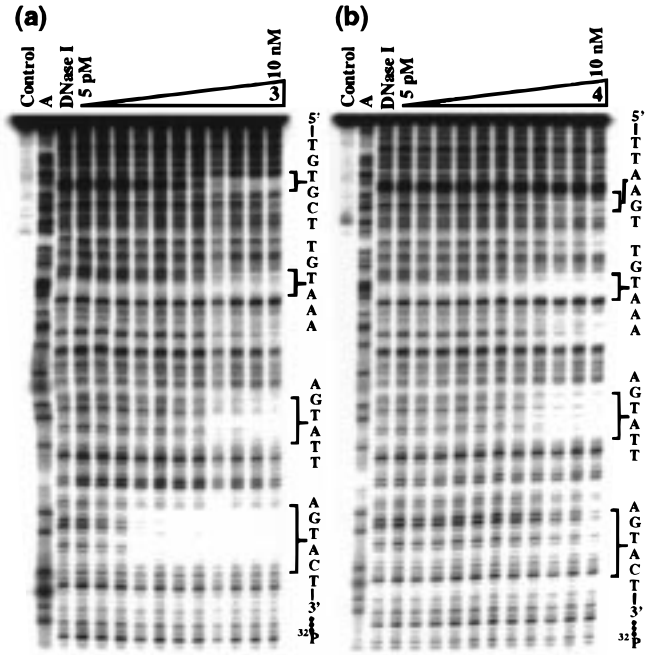

Figure 7. Quantitative DNase I footprint titration experiments with (a) cyclo-(γ-ImPyPyPy-(*R*)^{H2N}γ-ImPyPyPy) (**3**) and (b) cyclo-(γ-ImPyPyPy-(*R*)^{H2N}γ-PyPyPyPy) (**4**) on the 3′-end labeled 229 base pair restriction fragment: lane 1, intact; lane 2, A reaction; lane 3, DNase I standard; lanes 4−14, 5 pM, 10 pM, 20 pM, 50 pM, 100 pM, 200 pM, 500 pM, 1 nM, 2 nM, 5 nM, and 10 nM. The 5′-AGTACT-3′ and 5′-AGTATT-3′ sites were analyzed and are shown on the right side of the autoradiogram. Additional sites not analyzed are 5′-TGTAAA-3′, 5′-TGTGCT-3′, and 5′-TTAAGT-3′. All reactions contain 20 kcpm restriction fragment, 10 mM Tris·HCl (pH 7.0), 10 mM KCl, 10 mM $MgCl_2$, and 5 mM $CaCl_2$.

Covalent coupling of dimer (**1**) to form hairpin polyamide (**2**) results in a 428-fold increase in the DNA binding affinity and comparable DNA binding sequence specificity. It is interesting to compare hairpin polyamide (**2**), ImPyPyPy-(*R*)^{H2N}γ-ImPyPyPy-OH, to the previously reported hairpin ImPyPyPy-γ-ImPyPyPy-β-Dp.[2a] Each hairpin contains eight aromatic rings and a single charge located either on the γ-turn or a C-terminal β-Dp group. Although hairpin polyamide (**2**) binds to DNA with affinity and specificity comparable to DNA

(20) Kent, S. B. H. *Annu. Rev. Biochem.* **1988**, *57*, 957.
(21) Barlos, K.; Chatzi, O.; Gatos, D.; Stravropoulos, G. *Int. J. Pept. Protein Res.* **1991**, *37*, 513.
(22) Sambrook, J.; Fritsch, E. F.; Maniatis, T. *Molecular Cloning*; Cold Spring Harbor Laboratory: Cold Spring Harbor, NY, 1989.
(23) For the treatment of data on cooperative association of ligands, see: Cantor, C. R.; Schimmel, P. R. *Biophysical Chemistry, Part III: the Behavior of Biological Macromolecules*; W. H. Freeman and Company: New York, 1980; p 863.

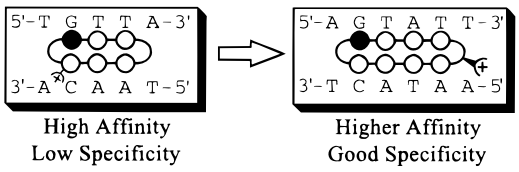

Figure 8. Comparison of first-generation six-ring cycle polyamide,[10] and second generation eight-ring cycle polyamide described here. Schematic binding model is as described in Figure 1.

binding proteins, it does bind with 4-fold lower affinity and 5-lower sequence specificity than the previously described hairpin ImPyPyPy-γ-ImPyPyPy-β-Dp. This probably results from loss of favorable interactions between the β-Dp group and A,T rich flanking sequences.[8b] Since cycle polyamides have no C-terminal β-Dp group, hairpin polyamide (**2**) is a more applicable control for the study described here.

On the basis of the pairing rules for polyamide−DNA complexes, the 5′-AGTACT-3′ and 5′-AGTATT-3′ sites represent "match" and "single base pair mismatch" sites for cycle-**3**, respectively, and "single base pair mismatch" and "match" sites for cycle-**4**, respectively. Cycle polyamide (**3**), cyclo-(γ-ImPyPyPy-$(R)^{H2N}\gamma$-ImPyPyPy), binds the six base pair 5′-AGTACT-3′ target sequence with an equilibrium association constant, $K_a = 7.6 \times 10^{10}$ M^{-1}, and 55-fold specificity over the single base pair mismatch 5′-AGTA*T*T-3′ site ($K_a = 1.3 \times 10^9$ M^{-1}). These affinities represent a 3600-fold increase relative to dimer (**1**) and an 8-fold enhancement relative to hairpin polyamide (**2**). Furthermore, the affinity and specificity of (**3**) are comparable to those of the previously described hairpin ImPyPyPy-γ-ImPyPyPy-β-Dp. The cycle polyamide (**4**), cyclo-(γ-ImPyPyPy-$(R)^{H2N}\gamma$-PyPyPyPy), which contains a single Im/Py pair, preferentially binds the 5′-AGTATT-3′ match site ($K_a = 3.1 \times 10^9$ M^{-1}) versus the single base pair mismatch 5-AGTACT-3′ ($K_a = 4.2 \times 10^8$ M^{-1}) with a 7-fold preference. Therefore, replacing a single pyrrole amino acid in cyclo-(γ-ImPyPyPy-$(R)^{H2N}\gamma$-PyPyPyPy) (**4**) with an imidazole residue in cyclo-(γ-ImPyPyPy-$(R)^{H2N}\gamma$-ImPyPyPy) (**3**), regulates cycle polyamide specificity and affinity by 2 orders of magnitude (see Figure 7).

Conclusions. A second generation cycle polyamide motif has been designed and characterized. Two eight-ring (-γ-4-γ-4-) cycle polyamides were found here to bind to DNA with affinity and specificity comparable to naturally occurring DNA binding proteins. The polyamide DNA binding affinity increases as expected as the number of consecutive ring pairings increases from 3 to 4.[9a] Important key design factors likely contributed to the improved specificity of the 8-ring cycles compared with the original design (Figure 8).[10] Moving the charge to the γ-turn may enhance the cycle polyamide binding orientation preference and hence binding-specificity. Determination of the exact molecular basis for the optimization of the cycle polyamides awaits further footprinting efforts as well as high resolution structure studies. However, it is clear from comparison of first and second generation cycles that polyamide design for DNA recognition can be continually optimized using affinity and *specificity* as two key criteria in parallel with continued investment in synthetic methodology.

Experimental Section

Dicyclohexylcarbodiimide (DCC), Hydroxybenzotriazole (HOBt), 2-(1H-benzotriazole-1-yl)-1,1,3,3-tetramethyluronium hexafluorophosphate (HBTU); aminomethylated polystyrene, 4-(bromomethyl)phenylacetic acid phenacyl ester, and 0.6 mmol/gram Boc-β-alanine-(4-carboxamidomethyl)-benzyl-ester-copoly(styrene-divinylbenzene) resin (Boc-β-Pam resin) was purchased from Peptides International (0.2 mmol/gram) (*R*)-2-Fmoc-4-Boc-diaminobutyric acid, and (*R*)-2-amino-4-Boc-diaminobutyric acid were from Bachem. *N*,*N*-diisopropylethylamine (DIEA), *N*,*N*-dimethylformamide (DMF), *N*-methylpyrrolidone (NMP), DMSO/NMP, acetic anhydride (Ac_2O), and 0.0002 M potassium cyanide/pyridine were purchased from Applied Biosystems. Dichloromethane (DCM) and triethylamine (TEA) were reagent grade from EM, thiophenol (PhSH) and dimethylaminopropylamine (Dp) were from Aldrich, trifluoroacetic acid (TFA) Biograde was from Halocarbon, phenol was from Fisher, and ninhydrin was from Pierce. All reagents were used without further purification. Quik-Sep polypropylene disposable filters were purchased from Isolab, Inc. A shaker for manual solid-phase synthesis was obtained from St. John Associates, Inc. Screw-cap glass peptide synthesis reaction vessels (5 mL and 20 mL) with a no. 2 sintered glass frit were made as described by Kent.[20] ^{1}H NMR spectra were recorded on a General Electric-QE NMR spectrometer at 300 MHz with chemical shifts reported in parts per million relative to residual solvent. UV spectra were measured in water on a Hewlett-Packard model 8452A diode array spectrophotometer. Optical rotations were recorded on a JASCO Dip 1000 digital polarimeter. Matrix-assisted, laser desorption/ionization time-of-flight mass spectrometry (MALDI-TOF) was performed at the Protein and Peptide Microanalytical Facility at the California Institute of Technology. HPLC analysis was performed on either a HP 1090M analytical HPLC or a Beckman Gold system using a RAINEN C18, Microsorb MV, 5μm, 300 × 4.6 mm reversed phase column in 0.1% (wt/v) TFA with acetonitrile as eluent and a flow rate of 1.0 mL/min, gradient elution 1.25% acetonitrile/min. Preparatory reversed phase HPLC was performed on a Beckman HPLC with a Waters DeltaPak 25 × 100 mm, 100 μm C18 column equipped with a guard, 0.1% (wt/v) TFA, 0.25% acetonitrile/min. Water (18Ω) was obtained from a Millipore MilliQ water purification system, and all buffers were 0.2 μm filtered.

Resin Substitution. Resin substitution can be calculated as L_{new}-(mmol/g) = $L_{old}/(1 + L_{old}(W_{new} - W_{old}) \times 10^{-3})$ (eq 2), where L is the loading (mmol of amine per gram of resin), and W is the weight ($gmol^{-1}$) of the growing polyamide attached to the resin.[21]

Control Hairpin ImPyPyPy-$(R)^{H2N}\gamma$-ImPyPyPy-C3−OH (2). ImPyPyPy-$(R)^{Fmoc}\gamma$-ImPyPyPy-β-Pam resin was synthesized in a stepwise fashion by machine-assisted solid-phase methods from Boc-β-alanine-Pam resin (0.6 mmol/g).[13] (*R*)-2-Fmoc-4-Boc-diaminobutyric acid (0.7 mmol) was incorporated as previously described for Boc-γ-aminobutyric acid. ImPyPyPy-$(R)^{Fmoc}\gamma$-ImPyPyPy-β-Pam resin was placed in a glass 20-mL peptide synthesis vessel and treated with DMF (2 mL), and then with piperidine (8 mL) and agitated (22 °C, 30 min). ImPyPyPy-$(R)^{H2N}\gamma$-ImPyPyPy-β-Pam resin was isolated by filtration and washed sequentially with an excess of DMF, DCM, MeOH, and ethyl ether, and the amine resin was dried in vacuo. A sample of resin (200 mg 0.40 mmol/gram) was suspended in absolute ethanol (25 mL). $LiBH_4$ (200 mg) was added and the mixture refluxed for 16 h. The reaction mixture was then filtered to remove resin, neat TFA was added (6 mL), and the resulting solution was concentrated in vacuo, resuspended in 0.1% (wt/v) TFA (8 mL), and purified twice by reversed phase HPLC to provide the trifluoroacetate salt of ImPyPyPy-$(R)^{H2N}\gamma$-ImPyPyPy-C3−OH (**2**) as a white powder upon lyophilization of the appropriate fractions: 2.5 mg, 3% recovery; ^{1}H NMR (DMSO-d_6) δ 11.03 (s, 1 H), 10.47 (s, 1 H), 10.13 (s, 1 H), 9.97 (s, 2 H), 9.94 (s, 1 H), 9.90 (s, 1 H), 8.35 (br s, 3 H), 8.29 (m 1 H), 8.01 (m, 1 H), 7.39 (s, 2 H), 7.32 (s, 1 H), 7.26 (m, 2 H), 7.22 (s, 1 H), 7.17 (m, 2 H), 7.08 (s, 2 H), 7.05 (s, 1 H), 7.02 (s, 2 H), 6.93 (s, 1 H), 6.84 (s, 1 H), 5.32 (m, 1 H), 3.98 (s, 6 H), 3.85 (s, 3 H), 3.83 (m, 9 H), 3.80 (s, 3 H), 3.78 (s, 3 H), 2.73 (m, 2 H), 2.35 (m, 2 H), 1.95 (m, 4 H), 1.73 (m, 2 H), MALDI-TOF-MS (monoisotopic) [M + H] 1139.5 (1139.5 calcd for $C_{53}H_{63}N_{20}O_{10}$).

Boc-Pyrrolyl-4-(oxymethyl)phenylacetic Acid Phenacyl Ester (5). A solution of Boc-Py acid (6.9 g, 29 mmol), 4-(bromomethyl)-phenylacetic acid phenacyl ester (10 g, 29 mmol), and DIEA (7.2 mL, 41 mmol) in 60 mL of DMF were stirred at 50 °C for 6 h. The solution was cooled and partitioned between 400 mL of water and 400 mL of ethyl ether. The ether layer was washed sequentially (2 × 200 mL each) with 10% citric acid, brine, saturated $NaHCO_3$, and brine. The organic phase was dried (sodium sulfate) and concentrated in vacuo.

The crude product was recrystallized from 3:1 ethyl acetate/hexanes to yield **5** as a fluffy white foam: 6.1 g, 42% yield; TLC (2:3 hexanes/ethyl acetate v/v) R_f 0.6 ^{1}H NMR (DMSO-d_6) δ 9.07 (s, 1 H), 7.90 (d, 2 H, J = 7.6 Hz), 7.61 (t, 1 H, J = 7.2 Hz), 7.50 (t, 2 H, J = 7.5 Hz), 7.31 (m, 4 H), 7.06 (s, 1 H), 6.62 (s, 1 H), 5.47 (s, 2 H), 5.16 (s, 2 H), 3.80 (s, 2 H), 3.76 (s, 3 H), 1.42 (s, 9H) ^{13}C NMR (DMSO-d_6) δ 193.1, 171.2, 160.6, 153.2, 135.7, 134.4, 130.1, 129.4, 128.5, 128.3, 123.7, 120.0, 119.0, 108.0, 79.0, 67.4, 65.1, 36.7, 28.6; FABMS *m*/*e* 506.205 (506.205 calcd for $C_{28}H_{30}N_2O_7$).

Boc-Pyrrolyl-4-(oxymethyl)phenylacetic Acid (6) Zinc dust was activated with 1 M HCl (aqueous) as described.[17] Boc-Pyrrolyl-4-(oxymethyl)phenylacetic acid phenacyl ester (3 g, 5.9 mmol) was dissolved in 90 mL 4:1 acetic acid/water (v/v). Zinc dust (9.6 g, 147 mmol) was added and the reaction stirred for 18 h at room temperature. The zinc was removed by filtration and the reaction mixture partitioned between 200 mL of ethyl ether and 200 mL of water. The layers were separated, the aqueous layer was extracted (ethyl ether, 1 × 200 mL), and the combined ether layers were washed (water, 5 × 100 mL), dried (sodium sulfate), concentrated in vacuo, and azeotroped (benzene, 6 × 100 mL). The crude acid product was purified by flash chromatography (2:1 hexanes/ethyl acetate) to yield a yellow oil: 2.0 g, 86% yield; TLC (ethyl acetate) R_f 0.7; ^{1}H NMR (DMSO-d_6) δ 9.06 (s, 1 H), 7.29 (d, 2 H, J = 7.8 Hz), 7.21 (d, 2 H. J = 7.8 Hz), 7.06 (s, 1 H), 6.6 (s, 1 H), 5.14 (s, 2 H), 3.74 (s, 3 H), 3.52 (s, 2 H), 1.38 (s, 9 H).

Boc-aminoacyl-Pyrrolyl-4-(oxymethyl)-Pam Resin (7). Boc-Pyrrolyl-4-(oxymethyl)phenylacetic acid (**6**) (1 g, 2.57 mmol) was dissolved in 6.5 mL DMF. HOBt (382 mg, 2.8 mmol) followed by DCC (735 mg, 3.2 mmol) was added and the reaction mixture shaken for 4 h at room temperature. The precipitated DCU was filtered and the reaction mixture was added to 10 g aminomethyl-polystyrene resin (0.7 mmol/g substitution) previously swollen for 30 min in DMF. DIEA (1 mL) was added and the reaction shaken until the resin was determined by the ninhydrin test and picric acid titration to be approximately 0.1 mmol/g substituted. The resin was washed with DMF, and the remaining amine groups were capped by acetylation (2×) with excess acetic anhyride capping solution (2:2:1 DMF/Ac_2O/DIEA). The resin was washed with DMF (1 × 20 mL), DCM (1 × 20 mL), and MeOH (1 × 20 mL) and dried in vacuo.

H_2N-γ-ImPyPyPy-(R)^{Boc}γ-PyPyPyPy-COOH (13). Cbz-γ-ImPyPyPy-(R)^{Fmoc}γ-PyPyPyPy-Pam resin was synthesized in a stepwise fashion by machine-assisted solid-phase methods from Boc-Py-Pam resin (0.1 mmol/g). (*R*)-2-Fmoc-4-Boc-diaminobutyric acid (0.7 mmol) was incorporated as previously described for Boc-γ-aminobutyric acid. Cbzγ-ImPyPyPy-(R)^{Fmoc}γ-PyPyPyPy-Pam resin was placed in a glass 20-mL peptide synthesis vessel and treated with DMF (2 mL) followed by piperidine (8 mL) and agitated (22 °C, 30 min). Cbzγ-ImPyPyPy-(R)^{H2N}γ-PyPyPyPy-Pam resin was isolated by filtration and washed sequentially with an excess of DMF, DCM, MeOH, and ethyl ether, and the amine resin was dried in vacuo. Cbzγ-ImPyPyPy-(R)^{H2N}γ-PyPyPyPy-Pam resin was then treated with 300 mg of Boc-anhydride (2 mL DMF, 1 mL DIEA, 55 °C, 30 min) to provide Cbzγ-ImPyPyPy-(R)^{Boc}γ-PyPyPyPy-Pam resin. Palladium acetate (200 mg, 37 °C, 10 min) in 2 mL of DMF was added to a sample of the Boc-resin (200 mg, 0.09 mmol/gram), ammonium formate (500 mg) was then added, and the reaction was allowed to shake for 8 h at 37 °C. The reaction mixture was then filtered to remove resin and precipitated palladium metal and diluted with 0.1% (wt/v) TFA (8 mL), and the resulting solution was purified by reversed phase HPLC to yield the trifluoroacetate salt of H_2N-γ-ImPyPyPy-(R)^{Boc}γ-PyPyPyPy-COOH: 17 mg, 66% recovery; ^{1}H NMR (DMSO-d_6) δ 10.35 (s, 1 H), 9.98 (s, 2 H), 9.96 (s, 3 H), 9.92 (s, 2 H), 7.98 (m, 1 H), 7.75 (br s 3 H), 7.44 (m, 1 H), 7.42 (s, 1 H), 7.30 (s, 1 H), 7.26 (s, 1 H), 7.25 (m, 2 H), 7.18 (m, 2 H), 7.15 (d, 1 H, J = 1.3 Hz), 7.13 (s, 1 H), 7.06 (m, 3 H), 6.96 (s, 1 H), 6.93 (s, 1 H), 6.90 (s, 1 H), 6.84 (d, 1 H, J = 1.8 Hz), 4.07 (q, 1 H, J = 6.0 Hz), 3.95 (s, 3 H), 3.84 (m, 15 H), 3.82 (s, 3 H), 3.79 (s, 3 H), 3.22 (m, 2 H), 2.81 (m, 2 H), 2.39 (t, 2 H, J = 6.9 Hz), 1.83 (m, 4 H), 1.39 (s, 9 H), MALDI-TOF-MS (monoisotopic) [M + H] 1281.5 (1281.6 calcd for $C_{60}H_{73}N_{20}O_{13}$).

H_2N-γ-ImPyPyPy-(R)^{Boc}γ-ImPyPyPy-COOH (12). Cbz-γ-ImPyPyPy-(R)^{Boc}-γ-ImPyPyPy-Pam resin was prepared as described for (**13**). A sample of the Boc-resin (330 mg, 0.09 mmol/gram) was treated with palladium acetate (330 mg, 37 °C, 10 min) followed by the addition of ammonium formate (500 mg, 37 °C, 8 h). The reaction mixture was then filtered to remove resin and diluted with 0.1% (wt/v) TFA (8 mL), and the resulting solution was purified by reversed phase HPLC to yield H_2N-γ-ImPyPyPy-(R)^{Boc}γ-ImPyPyPy-COOH as the trifluoroacetate salt: 4.2 mg, 10% recovery; ^{1}H NMR (DMSO-d_6) δ 10.36 (s, 1 H), 10.22 (s, 1 H), 10.14 (s, 1 H), 9.99 (s, 1 H), 9.97 (s, 2 H), 9.92 (s, 2 H), 7.97 (m, 1 H), 7.74 (br s 3 H), 7.45 (m, 1 H), 7.43 (s, 1 H), 7.42 (s, 1 H), 7.29 (s, 1 H), 7.26 (d, 1 H, J = 1.7 Hz), 7.23 (m, 2 H), 7.17 (s, 1 H), 7.14 (s, 1 H), 7.12 (s, 1 H), 7.06 (m, 2 H), 6.95 (s, 1 H), 6.90 (s, 1 H), 6.83 (d, 1 H, J = 1.3 Hz), 4.20 (m, 1 H), 3.94 (s, 6 H), 3.84 (m, 12 H), 3.81 (s, 3 H), 3.78 (s, 3 H), 3.22 (m, 2 H), 2.83 (quintet, 2 H, J = 6.2 Hz), 2.41 (t, 2 H, J = 6.9 Hz), 1.83 (m, 4 H), 1.38 (s, 9 H), MALDI-TOF-MS (monoisotopic) [M + H] 1282.6 (1282.6 calcd for $C_{59}H_{72}N_{21}O_{13}$).

Cyclo-(γ-ImPyPyPy-(R)^{H2N}γ-ImPyPyPy-) (3). The amine-polyamide **12** (2.8 mg, 2.0 μmol) was dissolved in DMF (7 mL), and treated with DPPA (12.5 μL) and K_2CO_3 (100 mg) for 3 h. The reaction mixture was concentrated in vacuo, treated with TFA (3 mL, 1 h), and purified by reversed phase HPLC to provide the trifluoroacetate salt of cyclo-(γ-ImPyPyPy-(R)^{H2N}γ-ImPyPyPy) (**3**). Cyclo-(γ-ImPyPyPy-(R)^{H2N}γ-ImPyPyPy) was recovered as a white powder upon lyophilization of the appropriate fractions (1.0 mg, 38% recovery). MALDI-TOF-MS (monoisotopic) [M + H] 1164.5 (1164.5 calcd for $C_{54}H_{62}N_{21}O_{10}$).

Cyclo-(γ-ImPyPyPy-(R)^{H2N}γ-PyPyPyPy) (4). The amine-polyamide **13** (7 mg, 5.0 μmol) was dissolved in DMF (7 mL), and treated with DPPA (12.5 μL) and K_2CO_3 (100 mg) for 3 h. The reaction mixture was concentrated in vacuo, treated with TFA (3 mL, 1 h), diluted to 8 mL with 0.1% (wt/v) TFA, and purified by reversed phase HPLC to provide cyclo-(γ-ImPyPyPy-(R)^{H2N}γ-PyPyPyPy) (**4**). Cyclo-(γ-ImPyPyPy-(R)^{H2N}γ-PyPyPyPy) was recovered as a white powder upon lyophilization of the appropriate fractions as the trifluoroacetate salt (2.6 mg, 41% recovery). ^{1}H NMR (DMSO-d_6) δ 10.56 (s, 1 H), 10.26 (s, 1 H), 9.96 (s, 2 H), 9.95 (s, 3 H), 9.92 (s, 1 H), 8.27 (m, 4 H), 9.00 (m, 1 H), 7.45 (s, 1 H), 7.39 (s, 1 H), 7.38 (s, 1 H), 7.34 (s, 1 H), 7.29 (s, 1 H), 7.26 (s, 1 H), 7.25 (s, 1 H), 7.18 (s, 1 H), 7.08 (s, 1 H), 6.93 (m, 1 H), 6.91 (s, 1 H), 6.89 (s, 1 H), 6.85 (s, 2 H), 6.82 (s, 1 H), 5.31 (m, 1 H), 3.93 (s, 3 H), 3.85 (s, 3 H), 3.83 (m, 9 H), 3.80 (s, 3 H), 3.78 (s, 3 H), 3.76 (s, 3 H), 3.23 (m, 2 H), 2.72 (m, 2 H), 2.36 (m, 2 H), 1.97 (m, 4 H), 1.38 (s, 9 H), MALDI-TOF-MS (monoisotopic) [M + H] 1163.4 (1163.5 calcd for $C_{55}H_{63}N_{20}O_{10}$).

Cyclo-(γ-ImPyPyPy-(R)$^{EDTA\cdot Fe(II)}$$\gamma$-PyPyPyPy-) (4-E·Fe(II)). Excess EDTA-dianhydride (180 mg) was dissolved in 1:1 DMSO/NMP (1 mL) and DIEA (1 mL) by heating at 60 °C for 10 min. The dianhydride solution was added to cyclo(γ-ImPyPyPy-(R)^{H2N}γ-PyPyPyPy-) (**4**) (1.3 mg, 1.0 μmol) dissolved in DMSO (1 mL). The mixture was heated (60 °C, 2 h) and the remaining EDTA-dianhydride hydrolyzed with 0.1M NaOH (2 mL, 60 °C, 15 min). Aqueous TFA (0.1wt %/v) was added to adjust the total volume to 8 mL and the solution purified directly by reversed phase HPLC to provide to cyclo-(γ-ImPyPyPy-(R)$^{EDTA\cdot Fe(II)}$$\gamma$-PyPyPyPy-) (**4-E·Fe(II)**) as a white powder upon lyophilization of the appropriate fractions: 0.25 mg, 18% recovery; MALDI-TOF-MS (monoisotopic) [M + H] 1438.1 (1437.6 calcd for $C_{65}H_{77}N_{22}O_{17}$).

DNA Reagents and Materials. Enzymes were purchased from Boehringer-Mannheim and used with their supplied buffers. Deoxyadenosine and thymidine 5′-[α-^{32}P] triphosphates were obtained from Amersham, and deoxyadenosine 5′-[γ-^{32}P]triphosphate was purchased from I. C. N. Sonicated, deproteinized calf thymus DNA was acquired from Pharmacia. RNase free water was obtained from USB and used for all footprinting reactions. All other reagents and materials were used as received. All DNA manipulations were performed according to standard protocols.[22]

Preparation of 3′- and 5′-End-Labeled Restriction Fragments. The plasmid pJT8 was constructed as previously reported. pJT8 was linearized with *Afl*II and *Fsp*I restriction enzymes, then treated with the Sequenase enzyme, deoxyadenosine 5′-α-^{32}P]triphosphate, and thymidine 5′-[α-^{32}P]triphosphate for 3′ labeling. Alternatively, these plasmids were linearized with *Afl*II, treated with calf alkaline phosphatase, and then 5′-labeled with T4 polynucleotide kinase and deoxyadenosine 5′-[γ-^{32}P]triphosphate. The 5′-labeled fragment was

then digested with *Fsp*I. The labeled fragment (3′ or 5′) was loaded onto a 6% nondenaturing polyacrylamide gel, and the desired 229 base pair band was visualized by autoradiography and isolated.

MPE·Fe(II) Footprinting.[14] All reactions were carried out in a volume of 400 μL. A polyamide stock solution or water (for reference lanes) was added to an assay buffer where the final concentrations were 20 mM HEPES buffer (pH 7.0), 10 mM NaCl, 100 μM/base pair calf thymus DNA, and 30 kcpm 3′- or 5′-radiolabeled DNA. The solutions were allowed to equilibrate for 4 h. A fresh 50 μM MPE·Fe(II) solution was prepared from 100 μL of a 100 μM MPE solution and 100 μL of a 100 μM ferrous ammonium sulfate ($Fe(NH_4)_2(SO_4)_2 \cdot 6H_2O$) solution. MPE·Fe(II) solution (5 μM) was added to the equilibrated DNA, and the reactions were allowed to equilibrate for 5 min. Cleavage was initiated by the addition of dithiothreitol (5 mM) and allowed to proceed for 14 min. Reactions were stopped by ethanol precipitation, resuspended in 100 mM Tris-borate-EDTA/80% formamide loading buffer, and denatured at 85 °C for 6 min, and a 5-μL sample (∼15 kcpm) was immediately loaded onto an 8% denaturing polyacrylamide gel (5% cross-link, 7 M urea) at 2000 V.

Affinity Cleaving.[15] All reactions were carried out in a volume of 400 μL. A polyamide stock solution or water (for reference lanes) was added to an assay buffer where the final concentrations were 20 mM HEPES buffer (pH 7.0), 20 mM NaCl, 100 μM/base pair calf thymus DNA, and 20 kcpm 3′- or 5′-radiolabeled DNA. The solutions were allowed to equilibrate for 8 h. A fresh solution of ferrous ammonium sulfate ($Fe(NH_4)_2(SO_4)_2 \cdot 6H_2O$) (10 μM) was added to the equilibrated DNA, and the reactions were allowed to equilibrate for 15 min. Cleavage was initiated by the addition of dithiothreitol (10 mM) and allowed to proceed for 30 min. Reactions were stopped by ethanol precipitation, resuspended in 100 mM tris-borate-EDTA/80% formamide loading buffer, and denatured at 85 °C for 6 min, and the entire sample was immediately loaded onto an 8% denaturing polyacrylamide gel (5% cross-link, 7 M urea) at 2000 V.

DNase I Footprinting.[16] All reactions were carried out in a volume of 400 μL. We note explicitly that no carrier DNA was used in these reactions until after DNase I cleavage. A polyamide stock solution or water (for reference lanes) was added to an assay buffer where the final concentrations were 10 mM Tris·HCl buffer (pH 7.0), 10 mM KCl, 10 mM $MgCl_2$, 5 mM $CaCl_2$, and 30 kcpm 3′-radiolabeled DNA. The solutions were allowed to equilibrate for a minimum of 12 h at 22 °C. Cleavage was initiated by the addition of 10 μL of a DNase I stock solution (diluted with 1 mM DTT to give a stock concentration of 1.875 u/mL) and was allowed to proceed for 7 min at 22 °C. The reactions were stopped by adding 50 μL of a solution containing 2.25 M NaCl, 150 mM EDTA, 0.6 mg/mL glycogen, and 30 μM base pair calf thymus DNA and then ethanol-precipitated. The cleavage products were resuspended in 100 mM Tris-borate-EDTA/80% formamide loading buffer, denatured at 85 °C for 6 min, and immediately loaded onto an 8% denaturing polyacrylamide gel (5% cross-link, 7 M urea) at 2000 V for 1 h. The gels were dried under vacuum at 80 °C and then quantitated using storage phosphor technology. Equilibrium association constants were determined as previously described.[12]

Acknowledgment. We are grateful to the National Institutes of Health (GM-27681) for research support, the National Institutes of Health for a research service award to D.M.H., J. Edward Richter for an undergraduate fellowship to J.M.T., and the Howard Hughes Medical Institute for a predoctoral fellowship to E.E.B. We thank G.M. Hathaway for MALDI-TOF mass spectrometry.

Supporting Information Available: Affinity-cleaving experiments of **4-E·Fe(III)** (PDF). This material is available free of charge via the Internet at http://pubs.acs.org.

JA983206X